

## REDUCTION OF AMPLITUDE AND DURATION OF POST-PULSE OSCILLATIONS IN BOW-TIE ACTIVE RADIATING ANTENNA

 Gennadiy P. Pochanin<sup>1</sup>,  Mikhail V. Nesterenko<sup>2\*</sup>,  Oleksandr A. Orlenko<sup>1</sup>,  Tetiana M. Ogurtsova<sup>1</sup>,  
 Iryna Ye. Pochanina<sup>1</sup>,  Vadym P. Ruban<sup>1</sup>

<sup>1</sup>*O.Ya. Usikov Institute for Radiophysics and Electronics of the National Academy of Sciences of Ukraine, 12, Ac. Proskura St., Kharkiv, Ukraine, 61085*

<sup>2</sup>*V.N. Karazin Kharkiv National University, 4, Svobody Sq., Kharkiv, Ukraine, 61022*

\*Corresponding Author e-mail: [mikhail.v.nesterenko@gmail.com](mailto:mikhail.v.nesterenko@gmail.com)

Received October 10, 2025; revised January 25, 2026; accepted February 7, 2026

The paper investigates one of the ways of suppressing post-pulse oscillations in ultra-wideband (UWB) electromagnetic pulses radiated by a bow-tie type antenna excited in active mode (the pulse generator is located directly on the radiator). Since this excitation method does not require balancing or other elements that match the impedances, conditions are created for increasing the radiated power with the same power consumption. To suppress post-pulse oscillations in the radiated field, resistive elements with high resistance are used. They are located near the excitation region in order to absorb the non-radiated part of the excitation signal energy accumulated in the antenna. The influence of the antenna form factor and load resistance on the shape of the radiated signal is experimentally analyzed.

**Keywords:** *UWB signal; Bow-Tie antenna; Radiated electromagnetic field; Post-pulse oscillations; Active antenna*

**PACS:** 02.70.Pt; 78.70.Gq; 84.37.+q; 84.40.Ba

### INTRODUCTION

One of the main applications of ultra-wideband (UWB) technologies is subsurface radar (ground penetrating radar (GPR)), which is widely used for such purposes as mine detection, detection of people by optically opaque obstacles, search for people under rubble, non-destructive testing of objects, environmental monitoring, monitoring the condition of subsurface communications, pipelines and many others (see, for example, [1]-[5] and references in them). Special requirements for the antenna system are imposed on GPR that use video pulses as UWB probing signals. The antenna must create in space a short single useful pulse of an electromagnetic field of the required amplitude, shape and duration. The presence of additional pulses in the probing signal (they are called post-pulse oscillations or ringing) complicates the interpretation of sounding results and deteriorates the information and accuracy characteristics of the GPR.

The most general is the use of dipole-type structures for impulse radiation. The prerequisite for the occurrence of post-pulse oscillations of the probing signal in such structures is the peculiarity of the very process of radiation of a single pulse by the antenna. The exciting signal goes from the exciting area to the ends of the dipole and back from the ends to the exciting area. Each propagation cycle in the antenna produces one impulse in the radiated field. It is impossible to create conditions under which all the energy supplied to the antenna is spent on radiating a single pulse during one pass of the exciting signal through the radiator [1]. Therefore, the portion of the non-radiated energy of the exciting signal propagating through the radiator and radiating at each cycle causes an appearance of post-pulse oscillations in the field created by the antenna. Depending on the geometry of the radiating elements and the electrophysical characteristics of the material from which they are made, a greater or lesser part of the energy supplied to the radiator is separated from the antenna, going into space. The remaining part continues to move along the radiator in the form of an electrical pulse, reflecting off the boundaries of the radiator and making oscillatory movements until the energy of the exciting signal is spent on the radiation of post-pulse oscillations, as well as on heating due to ohmic losses in the radiator and the return of part of the energy back to sources of the exciting signal.

One of the possible options for antenna structures for radiating UWB pulses are biconical dipoles, patented in 1898 by Lodge [6]. These can be symmetrical biconical dipoles with symmetrical excitation [7]-[19], asymmetrical biconical dipoles [20], [21] as well as biconical dipoles with asymmetrical excitation [22]. Calculations have shown that the use of specially formed resistive loading allows excluding post-pulse oscillations in radiated (received) signals. However, creating in practice such loadings is difficult.

A planar analogue of a biconical dipole is a dipole with triangular arms which is bow-tie antenna (BTA), also patented in [6]. It can be used both to generate harmonic electromagnetic fields [9], [23]-[34] and to radiate electromagnetic pulses [21], [35], [42]. Possible approach to prevent appearing of post-pulse oscillations and provide single pass propagation of exciting impulse by the antenna radiator is absorption of extra part of excitation energy by resistive or resistive-capacitive loads near the ends of dipole [35], [38].

The next update is the resistor-loaded bow-tie antenna, which is covered with a rectangular conducting cavity with inner walls partially or fully coated with a ferrite absorber [43]. This antenna is designed for GPR use. However, the

authors concluded that the ferrite absorber cannot significantly improve the antenna characteristics of the GPR system. The appearance of additional impulses in the radiated field is noted in the paper [39]. The dependence of the shape of the waveform of radiated impulse on the direction of radiation was also noted. It should be considered when designing an antenna for GPR.

The authors of the paper [21] show how the dimensions of a biconical antenna influence the radiation pattern and shape of radiated/received signals. The least influence is when the antenna dimensions are much bigger or much smaller than the central frequency of the signal. However, both of these cases have disadvantages from the practical point of view [44]. In [45], it was shown that cylindrical slots can radiate impulse signals due to an extensive working frequency band. Authors of [46] studied cylindrical radiator with six slots incising resistors. Specially designed distribution of resistors has shown to be a good performance in terms of absorbing ability at lower frequency, reflected pulse energy. However, the radiated/received pulses have long ringing after main pulse. Such signals require additional compressing to be applicable in GPR.

Active antennas, whose design includes active elements [47], are of particular interest to radar system developers. This approach improves the antenna's energy characteristics because it allows the abandonment of matching devices and significantly reduces signal energy losses at transmission from the generator to the radiator. It should be noted that the first radiators of electromagnetic (EM) waves, for example, [6], were active.

Earlier studies [48] showed that if the radiating elements of a BTA are used as a capacitive energy store for the further formation of a radiated pulse, then, in contrast to the passive method of antenna excitation, with the same parameters of the radiated pulse, in the case of active excitation, the energy consumed by the radiator, turns out to be an order of magnitude smaller.

Experiments for dipole allowed us to analyze the physical processes responsible for the radiation of EM fields. It was demonstrated that the area of excitation and the ends of the antenna are the main sources of intense radiation. By placing energy-absorbing resistors in the slots near the ends of the antenna arms, we reduce the radiated energy by absorbing the electric current as it travels to the ends. Therefore, it makes sense to absorb the excess energy from the exciting signals after they have been radiated from the ends of the antenna arms [2].

This paper proposes a design of a BTA that provides efficient radiation and simultaneously suppresses post-pulse oscillations. Electrodynamic characteristics of UWB bow-tie radiators of various shapes with resistive loads of different values are theoretically and experimentally investigated.

## FDTD SIMULATION

### 1. Problem Formulation

Unfortunately, active antennas are difficult to model mathematically. The result is influenced not only by the geometry and material of the radiator but also by the electrical parameters of the excitation circuit, together with active electronic elements (usually semiconductor diodes, transistors, etc.), and the feedback caused by these parameters. With this in mind, we will first find out the main regularities of pulse radiation caused by the geometry of the radiating elements based on the results of finite-difference time-domain (FDTD) modeling. Then, in the experimental part of the work, we will connect the radiator to the circuit generating exciting pulses and select its parameters that provide the desired radiation mode. In contrast to the approach of using a resistive load proposed in [38], in this study, a resistive load designed to suppress after-pulse oscillations is moved to the excitation region of the radiator.

Consider a BTA (Fig. 1) located in free space. Triangular conductors are located in the  $xz$ -plane. The dipole axis is oriented in the  $x$ -direction. The antenna dimensions: length is  $h_1$ , width is  $h_2$ . The antenna is excited by a unipolar pulse through the terminals "1". The exciting source is located in the center of the Cartesian coordinate system in the gap between the antenna conductors. Connected to the terminals "2" the load is resistive elements, the resistances of which are selected during the study in the range from 100 Ohms to 1000 Ohms.

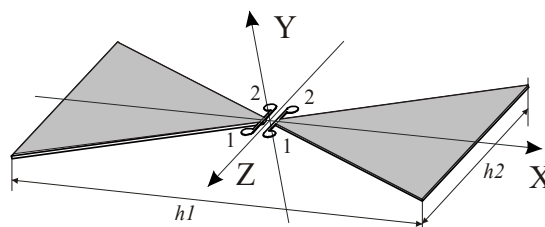


Figure 1. BTA: 1, 2 - antenna feeding and load terminals

Let us analyze the amplitude-time characteristics of the EM field registered at some distance  $h$  from the radiator in the direction of the  $y$  axis, depending on the dimensions  $h_1$ ,  $h_2$  and the value of the resistive load.

### 2. Solution Method

The mathematical statement of the problem includes the main equations, which are Maxwell's equations and initial and boundary conditions (to limit the calculation area and effectively use numerical methods). One of the most universal

and common methods of numerically solving non-stationary electrodynamics problems is the FDTD method [49]. We will use the specially developed program SEMP (Software for ElectroMagnetic Profiling) [50] for computer simulation which implements it. Computer simulation of the radiation of fully three-dimensional antennas using the FDTD method is a task that requires large amounts of calculations and resources. However, there are "optimization techniques" that allows to increase the speed of calculations, namely: 1) the use of a point model of the antenna excitation source, which simplifies the calculation algorithm and allows to use a larger size of the discretization grid than in the case of a full 3D model; 2) application of effective absorbing boundary conditions (ABC) [51].

### 3. Simulation Parameters

When limiting the computational domain in the FDTD method, the following two conditions must be considered: 1) the calculation area should have as small a volume as possible to increase the speed of calculations and reduce the amount of memory used; 2) the dimensions of the calculation area should be chosen so that reflections from its boundaries (taking into account the application of ABC) do not distort the investigated electromagnetic process. The simulation parameters related to the features of the implementation of the FDTD algorithm are given in Table I.

Table I. Simulation Parameters

Parameter	Value
Dimensions of the calculation area in space, m <sup>3</sup>	0.7×0.35×0.35
The size of the spatial grid, m	0.0025
Time window (observation time), ns	6
The time step, ns	10 <sup>-2</sup>

### 4. Simulation Results

Fig. 2 visualizes the distribution of the EM field radiated by the investigated rectangular ( $h_1=2$   $h_2=130$  mm) unloaded antenna in space in discrete time intervals. Field distributions at different moments are presented on images in the  $xz$ -plane. The color scale shows the amplitudes of the field strengths.

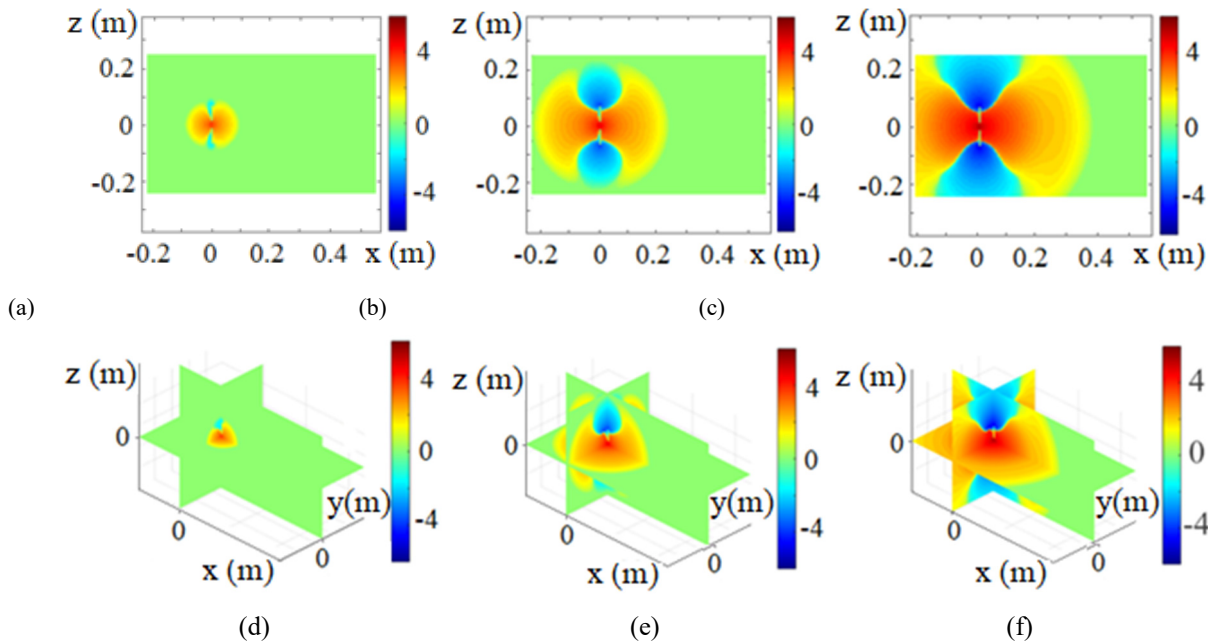
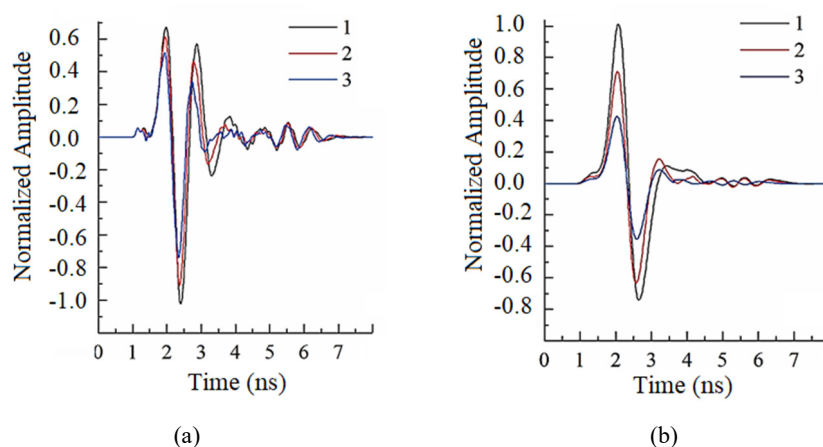


Figure 2. Distribution of the EM field radiated by a rectangular ( $h_1=2$   $h_2=130$  mm) unloaded BTA in the  $xz$ -plane (a), (b), (c) and in space (d), (e), (f) for some  $t$ : (a), (d) – 0.5 ns; (b), (e) – 1.0 ns; (c), (f) – 1.5 ns

Fig. 2 illustrates that the amplitudes of EM field pulses near the center of the antenna and at its edges are the most significant. This confirms the thesis that the primary sources of EM field radiation are the areas where the charges excited by the source receive the greatest acceleration.

Fig. 3 shows that an unloaded antenna radiates pulses with post-pulse oscillations of much higher intensity than a loaded one. An increase in the antenna length from 110 mm to 150 mm leads to an increase in the intensity of the radiated field (see the amplitude in Fig. 3a at the time interval of 1 ns–3 ns). This part of the pulse is formed during radiation directly from the excitation area. Since the length of the antenna is less than the spatial duration of the exciting pulse, the fields radiated by the edges of the antenna and having the opposite polarity arrive at the observation point at a time when the intensity of the field radiated by the excitation area has not yet reached its maximum. As a result of such

synchronization in time, the fields radiated by the excitation area and the edges of the dipole mutually compensate each other, limiting the intensity of the field at the observation point. The process of forming the field pulse at the point of observation is similar to forming the radiated pulse by a dipole radiator [2]. Post-pulse oscillations are observed in the time interval  $2.5 \text{ ns} \div 6.0 \text{ ns}$ . The parameters of these oscillations weakly depend on the length of the radiator.



**Figure 3.** Plots of pulses radiated by a rectangular ( $h_1 = 2h_2$ ) BTA: FDTD simulation for unloaded (a) and loaded by the 200 Ohm resistance (b) antennas: 1 –  $150 \times 75$  mm; 2 –  $130 \times 65$  mm; 3 –  $110 \times 55$  mm

However, such synchronization, in addition to the increase in field strength at the point of observation, creates conditions for the occurrence of post-pulse oscillations that follow this (negative) amplitude peak. As a result, the radiated field takes the form of a damped oscillation (Fig. 3a,  $3 \text{ ns} \div 5 \text{ ns}$ ). Despite the increase in amplitude, this form of probing signal is inconvenient for use in ground-penetrating radars. With this in mind, this paper proposes suppressing post-pulse oscillations by connecting a load resistor in the excitation region parallel to the excitation signal's source. The result of applying such a load in FDTD modeling is shown in Fig. 3b. A significant decrease in the amplitude of post-pulse oscillations in the radiated pulse is clearly visible. The resistive load connected in the excitation region reduces the Q-factor of the oscillations in the antenna. Despite the coincidence of the length of the antenna with the spatial duration of the pulse, there are no fading oscillations in the radiation field of the antenna with a length of  $h_1 = 150$  mm.

### EXPERIMENTAL RESEARCH

The object of research in this paper is an active radiating antenna that is excited without the use of a feeder line between the generator and the radiator (Fig. 4a). It is obvious that the addition of elements of electric circuits to the excitation region of the dipole significantly affects the shape of the radiated pulse. Therefore, the influence of the electrical parameters of the pulse generator output on the processes of formation and flow of the exciting current in the antenna should be taken into account.

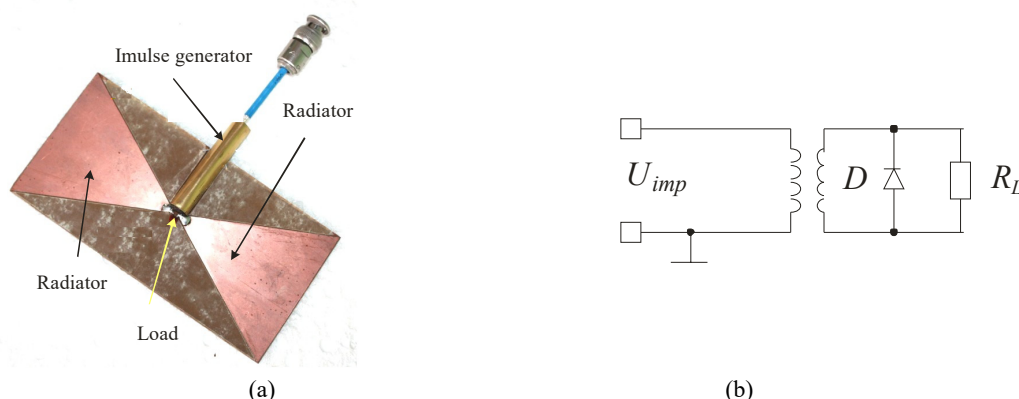


**Figure 4.** Appearance of an active antenna with a radiator of rectangular configuration (a); the output part of the pulse generator with a resistive load (b)

To find out the conditions under which both a large amplitude of the radiated field and a minimization of post-pulse oscillations are simultaneously achieved, it is advisable to conduct direct experiments on the radiation of short pulses of the EM field by active BTA with different radiator geometries. The study considered two configurations of the radiator - rectangular ( $h_1 = 2h_2$ ) and square ( $h_1 = h_2$ ). Let's analyze the influence of the load resistance, which is connected to the excitation area, on the pulse parameters of the radiated field. To do this, we connect the arms of the dipole in the region of excitation with resistance  $R_L$  (Fig. 4b). Resistors whose resistance is  $100 \text{ Ohm} \div 1000 \text{ Ohm}$  are used as load elements.

### 1. Measuring equipment

Fig. 5a contains an oscilloscope with a sweep block unit and an amplifier working in the 0÷3.5 GHz frequency range; timing generator, which generates a signal with an amplitude of +5 V and a duration of at least 20 ns to start the antenna excitation pulse generator and the oscilloscope synchronization signal; the power supply unit of the excitation pulse generator, which provides a voltage of +12 V and a current of 25 mA.

A ferrite antenna [52] was used as a receiving antenna, which allows receiving pulse signals with a rise time of more than 0.4 ns and a pulse duration of less than 2.5 ns without distortion. Registration of radiated pulses of the EM field is carried out at a distance of 0.5 m from the investigated antenna at a height of 1.8 m from the floor surface. This combination of distances makes it possible to exclude pulses reflected from surrounding objects (floor, walls, ceiling of the laboratory, measuring equipment) from the observation time window. Thus, the conditions of the experiment make it possible to analyze the structure of the radiated field and the effect on it of the design parameters of the radiator.

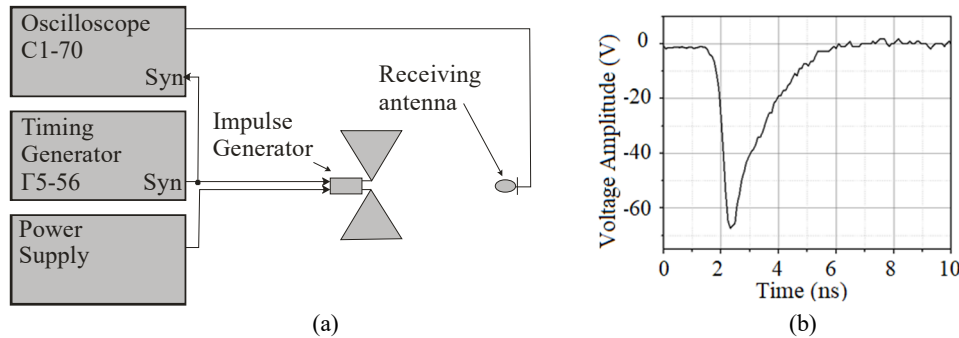


Figure 5. Block diagram of the experimental equipment (a) and exciting pulse at the output of the generator load 50 Ohm (b)

To excite the radiator, a pulse generator was developed [53] using a diode КД513А, which acts as a drift diode with a sharp recovery of resistance [54] and allows forming of a pulse with a front duration of 0.5 ns and amplitude of 70 V at a load of 50 Ohm (Fig. 5b). Structurally, the generator is made in the form of a shielded printed circuit board with dimensions of 50x10 mm<sup>2</sup>, located directly on the radiator (Fig. 4a). Since the generator has its own timing circuits, as well as a stabilized power source, the parameters of the generated voltage pulse do not depend on the duration of the start signal. The input signal for starting the generator is a pulse of positive polarity with an amplitude of 5 V and an arbitrary duration (from 20 ns or more). The supply voltage is +12 V, and the average current consumption is 25 mA at a pulse repetition rate of 100 KHz.

### 2. Radiation of pulses of EM fields

For experiments (antenna with a dipole aspect ratio of 2:1), radiators with dimensions  $h_l$  of 150 mm, 140 mm, 130 mm, 120 mm, and 110 mm were made. During the experiments, the time dependences of electromagnetic field pulses radiated by unloaded and loaded ( $R_L = 200$  Ohm) antennas were recorded (Fig. 6). The plots of the received signals clearly demonstrate that the load connection practically eliminates the post-pulse oscillations. However, the amplitude of the radiated pulse decreases by almost 1.5 times. The first two half-waves of the signal, which have the maximum amplitude, will be considered a "useful" signal. Let's define its amplitude as  $V_A = V(t)_{\max} + |V(t)_{\min}|$ . Consider it as the value of the amplitude for the useful signal (range  $t \in \{1, 3, 5\}$  ns in Fig. 6a) and the amplitude of after-pulse oscillations (range  $t \in \{3, 5, 12\}$  ns in Fig. 6b).

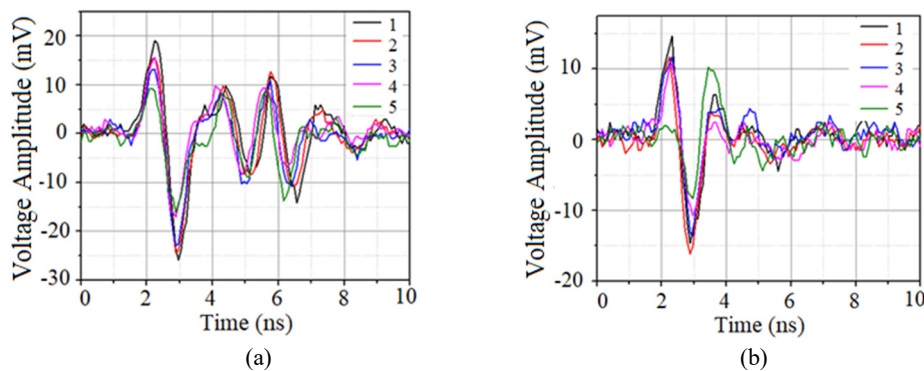


Figure 6. Plots of pulses radiated by an antenna of a rectangular configuration without load (a) and with load (b)  $R_L = 200$  Ohm: 1 – 150 mm; 2 – 140 mm; 3 – 130 mm; 4 – 120 mm; 5 – 110 mm

### 3. Effect of antenna size and load magnitude

From Fig. 6, it can be seen that with each decrease in the size of  $h_1$  by 10 mm, the amplitude of the useful signal decreases by approximately 4 mV for an unloaded antenna (Fig. 6a) and by 2 mV for a loaded antenna (Fig. 6b) for  $h_1$  sizes of the radiator from 150 mm to 110 mm. This means that the dependence of the amplitude of the useful signal on the size of  $h_1$  in these cases is linear (Fig. 7) and has the form:

$$V_A \approx 0.4 h_1 - 0.015 \text{ --for the unloaded antenna;}$$

$$V_A \approx 0.2 h_1 \text{ --for the loaded antenna.}$$

In addition, from Fig. 6, it can be seen that the amplitude of post-pulse oscillations changes slightly for both unloaded (Fig. 6a) and loaded (Fig. 6b) antennas, while signal amplitudes change significantly when the radiator size changes (Fig. 7).

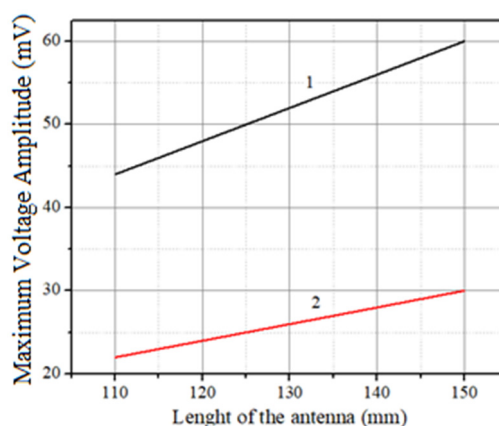


**Figure 7.** The amplitude of the useful signal depending on the size of the antennas (1 - no load, 2 - with a load  $R_L = 200$  Ohm)

Compare the plots of pulses emitted by rectangular antennas with a load magnitude ( $R_L = 200$  Ohm) and without a load at the same size as the radiators in the time interval from 5 ns to 9 ns (see Fig. 6). To quantify the impact of the load on the radiated signal, consider the amplitude of the first two half-waves that follow the radiated useful pulse. Fig. 8 shows the dependence of the amplitude of the useful pulse and two half-waves of post-pulse oscillations on the load resistance of the antennas, which was changed from 100 Ohm to 1000 Ohm in steps of 100 Ohm. A radiator of length  $h_1 = 130$  mm was chosen for this experiment.

From Fig. 8, it follows that when the load resistance increases from 100 Ohm to 300 Ohm, the amplitude of the useful signal increases faster than the amplitude of post-pulse oscillations. When the load increases from 300 Ohm to 1000 Ohm, the amplitudes of the useful pulse and post-pulse oscillations change similarly. Moreover, the amplitude of the first half-wave decreases (Fig. 8, curve 2), and the amplitude of the second half-wave (Fig. 8, curve 3) increases. When the resistance increases to 1000 Ohm, the amplitude of the useful pulse and post-pulse oscillations slowly increases to the values formed by the antenna without load. Thus, by applying a resistive load (from 200 Ohm to 300 Ohm) in active BTA with a rectangular configuration, it is possible to significantly (up to -20 dB) reduce the amplitude of after-pulse oscillations, while the amplitude of the useful signal decreases by only (20 ÷ 30) %.

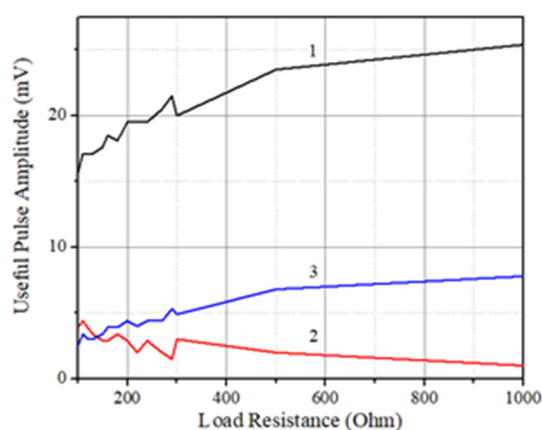


**Figure 8.** Dependence of the amplitude of the useful pulse and two half-waves of after-pulse oscillations on the antenna load: 1 is the amplitude of useful signal, 2 is the amplitude of the first half-wave, 3 is the amplitude of the second half-wave

#### 4. Antenna with a 1:1 aspect ratio

For this series of experiments, radiators with dimensions  $h_1 = h_2$  of 150 mm, 140 mm, 130 mm, 120 mm, and 110 mm were manufactured. The experiments recorded the time dependences of EM field pulses radiated by unloaded and loaded ( $R_L = 200$  Ohm) antennas. Fig. 9 illustrates the results of the measurements. As can be seen, the characteristic features of the pulses radiated by the antenna with a rectangular configuration (Fig. 6) are repeated in the antenna with a square configuration (Fig. 9). Amplitudes of the useful signal (range  $t \in \{1, 4\}$  ns shown in Fig. 9a) and post-pulse oscillations (range  $t \in \{4, 20\}$  ns in Fig. 9b). From Fig. 9, it follows that the amplitude of post-pulse oscillations changes slightly within the certain limits of the change in size  $h_1$  for both unloaded (a) and loaded (b) antennas.

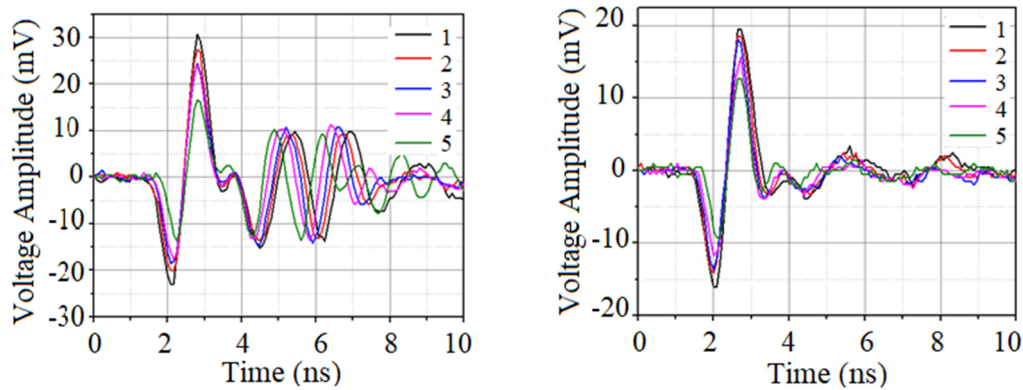


Figure 9. Plots of pulses radiated by a square antenna: without load (a), with load  $R_L = 200$  Ohm (b):  
 1 – 150 mm; 2 – 140 mm; 3 – 130 mm; 4 – 120 mm; 5 – 110 mm

#### 5. Effect of antenna size and load magnitude

From Fig. 10, it follows that with a decrease in the size of  $h_1$  by 10 mm, the maximum amplitude  $V_A$  of the useful signal decreases by about 6 mV for the unloaded antenna and by 4 mV for the loaded antenna in the range of sizes  $h_1$  of the radiator from 150 mm to 110 mm. This means that the dependence of the amplitude of the useful signal on the size of  $h_1$  within the limits of the change in the size of  $h_1$  is linear (Fig. 10) and is described by the expressions:

$$V_A \approx 0.6h_1 - 0.036 \text{ – for the unloaded antenna;}$$

$$V_A \approx 0.4h_1 - 0.014 \text{ – for the loaded antenna.}$$

Comparing the waveforms of Fig. 9 in the time interval from 5 ns to 9 ns reveals that the use of a resistor of  $R_L = 200$  Ohm allows significantly reducing the amplitude of the EM wave reflected from the ends of the antenna (up to -20 dB). Still, simultaneously, the amplitude of the radiated pulse also decreases by (20 ÷ 40) %.

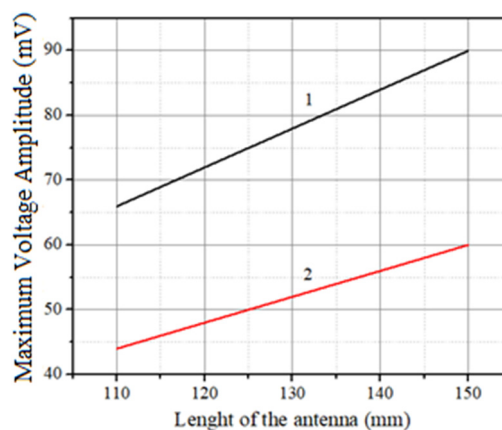
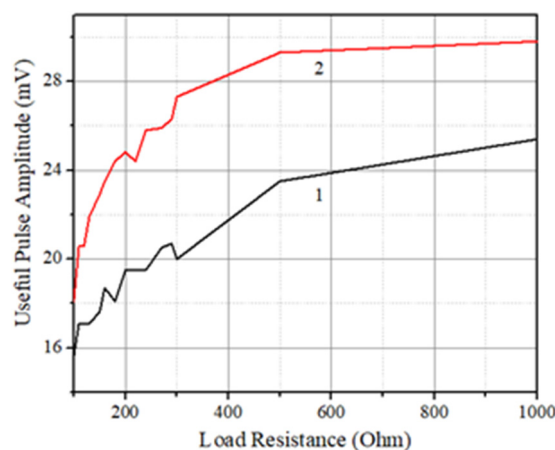


Figure 10. The amplitude of the useful signal depending on the dimensions of the antenna:  
 1 is for the unloaded antenna, 2 is for the antenna loaded by  $R_L = 200$  Ohm

#### 6. Comparison of radiators of rectangular and square configurations

Fig. 11 shows the dependence of the amplitudes of the useful pulse on the antenna load for radiators of rectangular and square configurations. Measurements were made for the radiators with a length of  $h_1 = 130$  mm. As you can see, that when using a resistive load, a square-shaped antenna radiates pulses of the EM field of greater amplitude than a rectangular

antenna with the same size  $h_1$ . With an increase in the load in the range of (100 ÷ 500) Ohm, the amplitude of the pulses radiated by a square-shaped antenna increases faster than that of a rectangular-shaped antenna. With a load close to 1000 Ohm, both antennas radiate pulses with the same useful pulse amplitude as an unloaded antenna of the corresponding size and shape.



**Figure 11.** Dependence of the amplitude of the useful pulse on the antenna load for radiators of rectangular and square configurations: 1 is for the rectangular  $h_2=65$  mm; 2 is for the square with  $h_2=130$  mm

From a comparison of the graphs shown in Fig. 6 and Fig. 9, it is evident that when the size of the radiator changes, the amplitude of the useful pulse changes significantly more than the amplitude of the after-pulse oscillations. This again confirms that field radiation is formed by areas where the charges excited in the antenna receive maximum acceleration - in the area of antenna excitation and at the edges of the radiator. In the case of an increase in the size of the antenna and a constant load, the radiating edges of the antenna move apart, and the time interval between radiation from the feeding region of the antenna and from the edge increases, this delays the appearance of the pulse radiated by the edge in the observation point. Since the electric field strength vectors radiated by the feeding region and the edge of the radiator have mutually opposite directions [48] and mutually compensate each other, increasing the time interval between these pulses makes it possible to increase the field strength of the pulse radiated by the feeding region to greater values before a compensating pulse arrives at the point of observation from the edge of the radiator. This is an explanation for the increase in the amplitude of the radiated field when the size of the radiator increases.

Since nothing changes in the feeding region with such changes in the antenna geometry, the after-pulse oscillations, most likely caused by radiation from this region, remain unchanged. However, if a resistor is included in the gap between the conductors of the dipole, which absorbs the energy of the excitation field wave reflected from the edge of the radiator, the energy of the excitation signal is mostly dissipated on this resistor and is not radiated.

### COMPARISON OF FDTD SIMULATION RESULTS AND EXPERIMENTAL DATA

The impulse signals registered in the experiments demonstrate the regularities revealed in the numerical simulation. Some discrepancy in the forms of program simulated and experimentally obtained pulses is explained by the presence of additional structural elements in experimental antenna samples that are not taken into account in numerical modeling (in particular, the "physical presence" of the generator, its imagined part of impedance and variable output resistance, a thin dielectric substrate on which the metal parts of the dipole are located, etc.).

The experiments revealed the following patterns:

- 1) with an increase in the size  $h_1$  of the antenna, the amplitude of the radiated signal increases more than the amplitude of post-pulse oscillations;
- 2) using resistors as a load significantly reduces the amplitude of the EM wave, which excites oscillations in the antenna; at that, the amplitude of the radiated pulse decreases slightly.

### CONCLUSIONS

The complex approach used in the paper (consideration of "simplified" theoretical and "full" experimental models) has its advantages. Simplification makes the theoretical model more universal and allows studying the basic regularities of signal formation and radiation without the influence of distorting factors. Considering the "full" experimental model allows for obtaining and analyzing the real spatial-temporal distributions of EM fields created by the antenna system under study. Thus, a complex approach, including theoretical (modeling) and experimental analysis, provides the most complete and effective study of the given experimental task. The mutual close correspondence of the results of calculations and experiments confirms the correctness of the chosen model and, as a result, opens up the possibility of an in-depth study of the dynamics of the change in the UWB pulse fields both in the near and far zones of the antenna.

As a result of the research, it was concluded:

- 1) from the point of view of practical use, square-shaped radiators are better than rectangular ones because the amplitude of the useful signal radiated by them is about 30% larger, and the post-pulse oscillations are the same as those of a rectangular-shaped radiator;
- 2) the largest efficiency of radiation at the minimum level of post-pulse oscillations is achieved if a load resistance of  $(200 \div 300)$  Ohm;
- 3) when using a square radiator without load, the amplitude of the useful pulse depends only on the length of the dipole. In contrast, the amplitude of post-pulse oscillations is almost independent on the length of the dipole.

Thanks to the active mode of antenna excitation, the need to match the impedance of the feeder and the radiator can be abandoned. So, there are no mismatch losses. This also opens the possibility of using resistive elements with arbitrary resistance to suppress oscillations in the radiator. So, it is possible to select the optimal load under which the post-pulse oscillations are minimal, and the amplitude of the radiated field pulse remains large.

#### ORCID

- ©Gennadiy P. Pochanin, <https://orcid.org/0000-0002-1977-2217>; ©Mikhail V. Nesterenko, <https://orcid.org/0000-0002-1297-9119>;  
©Oleksandr A. Orlenko, <https://orcid.org/0000-0002-3287-9692>; ©Tetiana M. Ogurtsova, <https://orcid.org/0000-0002-3211-4390>;  
©Iryna Ye. Pochanina, <https://orcid.org/0009-0002-3229-662X>; ©Vadym P. Ruban, <https://orcid.org/0000-0002-9008-7466>

#### REFERENCES

- [1] E. K. Miller, and J. A. Landt, "Direct time-domain techniques for transient radiation and scattering from wires," *Proc. IEEE*, **68**, (11), 1396-1423 (1980). <https://doi.org/10.1109/PROC.1980.11881>
- [2] G. P. Pochanin, and I. Ye. Pochanina, "Radiation of UWB pulses by thin wire monopole," in *Proc. 6th Int. Conf. Ultra Wideband and Ultra Short Impulse Signals*, 133-136 (2012). <https://doi.org/10.1109/UWBUSIS.2012.6379757>
- [3] L. A. Varyanitsa-Roshchupkina, and G. P. Pochanin, "Optimization of a sounding ultra wide-band (UWB) pulsed signal in subsurface object detection," *Telecom. Radio Eng.* **71**, 1159-1182 (2012). <https://doi.org/10.1615/telecomradeng.v71.i13.20>
- [4] G. P. Pochanin, and S. A. Masalov, "Large current radiators: problems, analysis, and design," in *Ultrawideband radar applications and design*. Ed. by J. D. Taylor. CRC Press. 325-372 (2012). <https://doi.org/10.1201/b12356>
- [5] O. A. Pryshchenko, V. A. Plakhtii, O. M. Dumin, G. P. Pochanin, V. P. Ruban, L. Capineri, and F. Crawford, "Implementation of an artificial intelligence approach to GPR systems for landmine detection," *Remote Sensing*, **14**, No. 17, 4421 (2022). <https://doi.org/10.3390/rs14174421>
- [6] O. Lodge, "Electric Telegraphy," U.S. Patent 609 154, Aug. 15, 1898.
- [7] S. A. Schelkunoff, "Theory of antennas of arbitrary size and shape," *Proc. IRE*, **29**, 493-521 (1941). <https://doi.org/10.1109/JRPROC.1941.231669>
- [8] C. T. Tai, "On the theory of biconical antennas," *Journal Applied Phys.* **19**, 1155-1160 (1948). <https://doi.org/10.1063/1.1715036>
- [9] G. H. Brown, and O. M. Woodward, "Experimentally determined radiation characteristics of conical and triangular antennas," *RCA Rev.*, **13**, 425-452 (1952).
- [10] J. Galejs, "Capacitor type biconical antennas," *Radio Science*, **68**, No. 2, 165-172 (1964).
- [11] T. T. Wu, and R. W. P. King, "The tapered antenna and its application to the junction problem for thin wires," *IEEE Trans. Antennas Propag.* **24**, 42-45 (1976). <https://doi.org/10.1109/TAP.1976.1141274>
- [12] S. A. Saoudy, and M. Hamid, "Input admittance of a biconical antenna with wide feed gap," *IEEE Trans. Antennas Propag.* **38**, 1784-1790 (1990). <https://doi.org/10.1109/8.102740>
- [13] S. S. Sandler, and R. W. P. King, "Compact conical antennas for wide-band coverage," *IEEE Trans. Antennas Propag.* **42**, 436-439 (1994). <https://doi.org/10.1109/8.280735>
- [14] K.-L. Wong, and S.-L. Chien, "Wide-band cylindrical monopole antenna for mobile phone," *IEEE Trans. Antennas Propag.* **53**, 2756-2758 (2005). <https://doi.org/10.1109/TAP.2005.851784>
- [15] A. K. Amert, and K. W. Whites, "Miniaturization of the biconical antenna for ultrawideband applications," *IEEE Trans. Antennas Propag.* **57**, 3728-3735 (2009). <https://doi.org/10.1109/TAP.2009.2026667>
- [16] C. S. Rao, and A. Sudhakar, "Analysis of edge terminated wide band biconical antenna," *ACES J.* **30**, 804-809 (2015).
- [17] M. V. Nesterenko, A. V. Gomofov, V. A. Katrich, S. L. Berdnik, and V. I. Kijko, "Scattering of electromagnetic waves by impedance biconical vibrators in a free space and in a rectangular waveguide," *Prog. Electromagn. Res. C*, **119**, 275-285 (2022). <http://dx.doi.org/10.2528/PIERC22020304>
- [18] F. F. Dubrovka, S. Piltyay, M. Movchan, and I. Zakharchuk, "Ultrawideband compact lightweight biconical antenna with capability of various polarizations reception for modern UAV applications," *IEEE Trans. Antennas Propag.* **71**, 2922-2929 (2023). <https://doi.org/10.1109/TAP.2023.3247145>
- [19] J. M. Platt, L. B. Boskovic, and D. S. Filipovic, "Wideband biconical antenna with embedded band-notch resonator," *IEEE Trans. Antennas Propag.* **72**, 2921-2925 (2024). <https://doi.org/10.1109/TAP.2024.3349785>
- [20] S. N. Samaddar, and E. L. Mokole, "Biconical antennas with unequal cone angles," *IEEE Trans. Antennas Propag.* **46**, 181-193, (1998). <https://doi.org/10.1109/8.660962>
- [21] D. Ghosh, and T. K. Sarkar, "Design of a wide-angle biconical antenna for wideband communications," *Prog. Electromagn. Res. B*, **16**, 229-245 (2009). <https://doi.org/10.2528/PIERB09061508>
- [22] M. V. Nesterenko, V. A. Katrich, and S. V. Pshenichnaya, "Multiband asymmetric biconical dipole antenna with distributed surface impedance and arbitrary excitation," *East European J. Physics*, (2), 450-455 (2024). <https://doi.org/10.26565/2312-4334-2024-2-59>
- [23] Y.-D. Lin, and S.-N. Tsai, "Coplanar waveguide-fed uniplanar bow-tie antenna," *IEEE Trans. Antennas Propag.* **45**, 305-306 (1997). <https://doi.org/10.1109/8.560350>

- [24] Y.-D. Lin, and S.-N. Tsai, "Analysis and design of broadside-coupledstriplines-fed bow-tie antennas," *IEEE Trans. Antennas Propag.* **46**, 459-460 (1998). <https://doi.org/10.1109/8.662667>
- [25] K. Kiminami, A. Hirata, and T. Shiozawa, "Double-sided printed bow-tie antenna for UWB communications," *IEEE Antennas Wireless Propag. Lett.* **3**, 152-153 (2004). <https://doi.org/10.1109/LAWP.2004.832126>
- [26] G. Wang, J. Liu, J. Xia, and L. Yang, "Coaxial-fed double-sided bow-tie antenna for GSM/CDMA and 3G/WLAN communications," *IEEE Trans. Antennas Propag.* **56**, 2739-2742 (2008). <https://doi.org/10.1109/TAP.2008.927571>
- [27] A. C. Durgun, C. A. Balanis, C. R. Birtcher, and D. R. Allee, "Design, simulation, fabrication and testing of flexible bow-tie antennas," *IEEE Trans. Antennas Propag.* **59**, 4425-4435 (2011). <https://doi.org/10.1109/TAP.2011.2165511>
- [28] H.-W. Liu, H. Jiang, X. Guan, J.-H. Lei, and S. Li, "Single-feed slotted bowtie antenna for triband applications," *IEEE Antennas Wireless Propag. Lett.* **12**, 1658-1661 (2013). <https://doi.org/10.1109/LAWP.2013.2294751>
- [29] X. Li, M. Jalilvand, Y. L. Sit, and T. Zwick, "A compact double-layer on-body matched bowtie antenna for medical diagnosis," *IEEE Trans. Antennas Propag.* **62**, 1808-1816 (2014). <https://doi.org/10.1109/TAP.2013.2297158>
- [30] T. Li, H. Zhai, X. Wang, L. Li, and C. Liang, "Frequency-reconfigurable bow-tie antenna for Bluetooth, WiMAX, and WLAN applications," *IEEE Antennas Wireless Propag. Lett.* **14**, 171-174 (2015). <https://doi.org/10.1109/LAWP.2014.2359199>
- [31] X. Zhang, C.-J. Chung, S. Wang, H. Subbaraman, Z. Pan, Q. Zhan, and R. T. Chen, "Integrated broadband bowtie antenna on transparent silica substrate," *IEEE Antennas Wireless Propag. Lett.* **15**, 1377-1381 (2016). <https://doi.org/10.1109/LAWP.2015.2510361>
- [32] J. Wang, Z. Shen, and L. Zhao, "Wideband dual-polarized antenna for spectrum monitoring systems," *IEEE Antennas Wireless Propag. Lett.* **16**, 2236-2239 (2017). <https://doi.org/10.1109/LAWP.2017.2709938>
- [33] Y. Shafiq, J. Henricks, C. P. Ambulo, T. H. Ware, and S. V. Georgakopoulos, "A battery-free temperature sensor with liquid crystal elastomer switching between RFID chips," *IEEE Access*, **8**, 87870-87883 (2020).
- [34] I. D. Chiele, M. Donelli, J. Iannacci, and K. Guha, "On chip modulated scattering tag operating at millimetric frequency band," *Prog. Electromagn. Res. C*, **124**, 71-77 (2024). <http://dx.doi.org/10.2528/PIERM23102707>
- [35] K. L. Shlager, G. S. Smith, and J. G. Maloney, "Optimization of bow-tie antennas for pulse radiation," *IEEE Trans. Antennas Propag.* **42**, 975-982 (1994). <https://doi.org/10.1109/8.299600>
- [36] Y. Nishioka, O. Maeshima, T. Uno, and S. Adachi, "FDTD analysis of resistor-loaded bow-tie antennas covered with ferrite-coated conducting cavity for subsurface radar," *IEEE Trans. Antennas Propag.* **47**, 970-977 (1999). <https://doi.org/10.1109/8.777119>
- [37] A. A. Lestari, A. G. Yarovoy, and L. P. Ligthart, "Ground influence on the input impedance of transient dipole and bow-tie antennas," *IEEE Trans. Antennas Propag.* **52**, 1970-1975 (2004). <https://doi.org/10.1109/TAP.2004.832371>
- [38] A. A. Lestari, A. G. Yarovoy, and L. P. Ligthart, "RC-loaded bow-tie antenna for improved pulse radiation," *IEEE Trans. Antennas Propag.* **52**, 2555-2563 (2004). <https://doi.org/10.1109/TAP.2004.834444>
- [39] F. Sagnard, D.-L. Ton, and J. Badet, "Analysis of the transient waveforms radiated by a combination of thin-wire antennas—part II: simulation results," *IEEE Antennas Wireless Propag. Lett.* **5**, 213-216 (2006). <https://doi.org/10.1109/LAWP.2006.875278>
- [40] D. Caratelli, and A. Yarovoy, "Unified time- and frequency-domain approach for accurate modeling of electromagnetic radiation processes in ultrawideband antennas" *IEEE Trans. Antennas Propag.* **58**, 3239-3255 (2010). <https://doi.org/10.1109/TAP.2010.2055800>
- [41] D. Lee, G. Shaker, and W. Melek, "A Broadband wrapped bowtie antenna for UWB pulsed radar applications," *IEEE Trans. Antennas Propag.* **68**, 7803-7812 (2020). <https://doi.org/10.1109/TAP.2020.3000556>
- [42] O. Fiser, V. Hruby, J. Vrba, T. Drizdal, J. Tesarik, J. Vrba Jr., and D. Vrba, "UWB bowtie antenna for medical microwave imaging applications," *IEEE Trans. Antennas Propag.* **70**, 5357-5372 (2022). <https://doi.org/10.1109/TAP.2022.3161355>
- [43] Y. Nishioka, O. Maeshima, T. Uno, and S. Adachi, "FDTD analysis of resistor-loaded bow-tie antennas covered with ferrite-coated conducting cavity for subsurface radar," *IEEE Trans. Antennas Propag.* **47**, 970-977 (1999). <https://doi.org/10.1109/8.777119>
- [44] G. P. Pochanin, "UWB/SP antennas classification," in: *Proc. Int. Symp. Physics and Engineering of Millimeter and Submillimeter Waves*, **3**, 549-550 (1994).
- [45] G. P. Pochanin and P. V. Kholod, "Cylindrical slot radiator of non-sinusoidal waves. Use of radio waves of millimeter and submillimeter ranges," Collection of scientific papers, Kharkiv: Institute for Radiophysics and Electronics of the National Academy of Sciences of Ukraine, 112-119 (1993).
- [46] D. Lee, G. Shaker, and W. Melek, "A broadband wrapped bowtie antenna for UWB pulsed radar applications," *IEEE Trans. Antennas Propag.* **68**, 7803-7812 (2020). <https://doi.org/10.1109/TAP.2020.3000556>
- [47] V. P. Prokhorenko, V. E. Ivashchuk, and S. V. Korsun, "Electromagnetic impulse radiator," in *Proc. 2nd Int. Conf. Ultra Wideband and Ultra Short Impulse Signals*, 244-245 (2004). <https://doi.org/10.1109/UWBUS.2004.1388115>
- [48] A.A. Orlenko, and P. V. Kholod, "Two modes of excitation of the UWB/SP transmitting antenna," in: *Proc. 3rd Int. Conf. Ultra Wideband and Ultra Short Impulse Signals*, (Sevastopol, Ukraine, 2006), pp. 185-187. <https://doi.org/10.1109/UWBUS.2006.307197>
- [49] A. Taflov, *Computational electrodynamics: The finite – difference time – domain method*, (New York: Artech House, 1995).
- [50] L. A. Varyanitzha-Roshchupkina, "Software for image simulation in ground penetrating radar problems," in: *Proc. 3rd Int. Conf. Ultra Wideband and Ultra Short Impulse Signals*, (Sevastopol, Ukraine, 2006), pp. 150-155. <https://doi.org/10.1109/UWBUS.2006.307172>
- [51] M. V. Nesterenko, S. L. Berdnik, A. V. Gomozyov, D. V. Gretsikh, and V. A. Katrich, "Approximate boundary conditions for electromagnetic fields in electromagnetics," *Radioelectronic and Computer Systems*, (3), 141-160 (2022). <https://doi.org/10.32620/reks.2022.3.11>
- [52] T.N. Ogurtsova, P.V. Kholod, and G.P. Pochanin, "Sensitivity of UWB ferrite receiving antennas," in: *Proc. 2nd Int. Conf. Ultra Wideband and Ultra Short Impulse Signals*, (Sevastopol, Ukraine, 2004), pp. 279-281. <https://doi.org/10.1109/UWBUS.2004.1388129>

- [53] O.A. Orlenko, "UWB pulse generators," in: *Proc. 6th Int. Conf. Ultra Wideband and Ultra Short Impulse Signals*, (Sevastopol, Ukraine, 2012), pp. 75-77. <https://doi.org/10.1109/UWBUSIS.2012.6379737>
- [54] V. Prokhorenko, V. Ivashchuk, S. Korsun, "Drift step recovery devices utilization for electromagnetic pulse radiation," in: *Proc. 10th Int. Conf. on Ground Penetrating Radar*, 195-198 (Piscataway, NJ, 2004). <https://doi.org/10.1109/ICGPR.2004.179954>

**ЗМЕНШЕННЯ АМПЛІТУДИ ТА ТРИВАЛОСТІ ПІСЛЯІМПУЛЬСНИХ КОЛИВАНЬ В АКТИВНІЙ  
ВИПРОМІНЮВАЛЬНІЙ АНТЕНІ ТИПУ «BOW-TIE»**

**Геннадій П. Почанін<sup>1</sup>, Михайло В. Нестеренко<sup>2</sup>, Олександр А. Орленко<sup>1</sup>, Тетяна М. Огурцова<sup>1</sup>,  
Ірина Є. Почаніна<sup>1</sup>, Вадим П. Рубан<sup>1</sup>**

<sup>1</sup>*Інститут радіофізики та електроніки ім. О.Я. Усикова Національної академії наук України,  
вул. Ак. Проскури, 12, м. Харків, Україна, 61085*

<sup>2</sup>*Харківський національний університет імені В.Н. Каразіна, майдан Свободи, 4, м. Харків, Україна, 61022*

У статті досліджується один із способів придушення післяімпульсних коливань у надширокопasmових (НШС) електромагнітних імпульсах, що випромінюються антеною типу «Bow-Tie», збудженою в активному режимі (генератор імпульсів розташований безпосередньо на випромінювачі). Оскільки цей метод збудження не вимагає балансування або інших засобів, необхідних для узгодження антени, створюються умови для збільшення випромінюваної потужності при тій самій споживаній потужності. Для придушення післяімпульсних коливань у випромінюваному полі використовуються резистивні елементи з високим опором. Вони розташовуються поблизу джерела збудження, щоб поглинути накопичену в антені невипромінену частину енергії. Експериментально проаналізовано вплив форм-фактора антени та опору навантаження на форму сигналу, що випромінюється.

**Ключові слова:** *надширокопasmовий сигнал; антена типу «Bow-Tie»; випромінюване електромагнітне поле; післяімпульсні коливання; активна антена*